Steady-State Analysis of Interaction Between Harmonic Components of Arm and Line Quantities of Modular Multilevel Converters

Kalle Ilves, *Student Member, IEEE*, Antonios Antonopoulos, *Student Member, IEEE*, Staffan Norrga, *Member, IEEE*, and Hans-Peter Nee, *Senior Member, IEEE*

***Abstract*—The fundamental frequency component in the arm currents of a modular multilevel converter is a necessity for the operation of the converter, as is the connection and bypassing of the submodules. Inevitably, this will cause alternating components in the capacitor voltages. This paper investigates how the arm currents and capacitor voltages interact when the submodules are connected and bypassed in a sinusoidal manner. Equations that describe the circulating current that is caused by the variations in the total inserted voltage are derived. Resonant frequencies are identified and the resonant behaviour is verified by experimental results. It is also found that the effective values of the arm resistance and submodule capacitances can be extracted from the measurements by least square fitting of the analytical expressions to the measured values. Finally, the analytical expression for the arm currents is verified by experimental results.**

***Index Terms*—Analytical steady-state model, arm currents, experimental results, modular multilevel converter, phase-leg resonance .**

NOMENCLATURE

$\hat{m}$	Modulation index.
ω	Fundamental frequency in radians per second.
ω_{rn}	Fundamental frequency in radians per second that causes resonance for the nth order harmonic.
ϕ_n	Angular displacement of the nth-order harmonic in the circulating current.
$\phi_{un,ln}$	Angular displacement of the nth-order harmonic in the upper- and lower-arm currents.
C	Submodule capacitance.
C_f	Capacitance of the dc-link filter.
i_n	Instantaneous value of the nth-order harmonic in the circulating current.
i_o	Instantaneous value of the ac-side current.
i_{dc}	Time average of the circulating current.
i_{a1}	Half of the instantaneous ac-side current.
$i_{cu,cl}$	Instantaneous capacitor current in the upper- and lower-arm submodules.
$i_{u,l}$	Instantaneous value of the upper- and lower-arm currents.
$i_{un,ln}$	Instantaneous value of the nth-order harmonic in the arm currents.
L	Total inductance in one phase leg.
N	Number of submodules per arm.
$N_{u,l}$	Upper and lower arm insertion indices.
R	Effective resistance of one phase leg.
s_{ref}	Reference waveform used to define angular displacements.
T	Fundamental frequency period in seconds.
t	Time in seconds.
u_n	Instantaneous value of the nth-order harmonic of the total inserted voltage in one phase leg.
$v_{cu,cl}$	Instantaneous capacitor voltages in the upper and lower-arm submodules.
$v_{iu,il}$	Instantaneous value of the inserted voltage by each submodule in the upper and lower arm.
$v_{u,l}$	Instantaneous value of the inserted voltage in the upper and lower arm.
Z_a	Total phase-leg impedance.
Z_f	Impedance of the dc-link filter.

Manuscript received February 16, 2011; revised May 11, 2011; accepted June 3, 2011. Date of current version December 16, 2011. Recommended for publication by Associate Editor B. Wu.

The authors are with the Department of Electrical Machines and Power Electronics Laboratory, Royal Institute of Technology, Teknikringen 33, SE-10044, Stockholm, Sweden (e-mail: ilves@kth.se; anta@kth.se; staffan.norrga@ee.kth.se; hansi@kth.se).

Digital Object Identifier 10.1109/TPEL.2011.2159809

I. INTRODUCTION

WITH the modular multilevel converter (M2C) a new era for high-power voltage source converters was entered. Since the M2C, which was first presented in [1]–[4], combines excellent output voltage waveforms with very high efficiencies [5], [6], it is ideal for high-voltage high-power applications such as high-voltage direct current transmission [5], [6], high-power motor drives [7]–[10], and electric railway supplies [11]. The basic operation [1]–[3], [12] and the internal dynamics [13] have been described, but no explicit analytical expressions for the arm currents have been presented so far. This holds for both the dynamics and for the steady-state case. The reason for this is that even a continuous representation of the circuit results in nonlinear equations.Explicit expressions for the arm currents and for their interaction with the arm voltages are a vital component for the understanding of the operation of the converter. Due to the aforementioned nonlinearities, harmonic components are inevitably generated in the arm quantities [14]. To predict the frequencies, the amplitudes, and the phase angles of these harmonic components, explicit expressions are very helpful. In the circuit-design stage an analytical representation is also helpful since voltage and current ratings depend

on the magnitudes of the harmonic components. However, the harmonic components can be influenced significantly by appropriate modifications of the control signals [15], and various control methods have therefore been suggested [13], [15]–[18]. Consequently, the steady-state control strategy is interrelated with the main-circuit design. Without an analytical representation, however, numerous time-consuming simulations have to be performed in order to find an adequate combination of circuit parameters and steady-state control signals. Additionally, an analytical steady-state representation of the arm quantities can also be helpful during the design of the dynamical control system. At first sight, this might seem strange because the design of the controllers is mainly based on the converter dynamics. Nevertheless, analytical steady-state equations may predict resonances that may dictate the boundaries for the controllers. If these boundaries can be expressed in terms of circuit parameters, the analytical expressions can very effectively describe the interrelations between main-circuit design, steady-state control, and dynamical controller design, and in this way the design process may be simplified substantially. It is, therefore, the intention of this paper to provide a complete set of analytical equations for the description of the arm quantities of an M2C, and to describe the interaction of arm currents, arm voltages, and phase-leg voltages.

The outline of the paper is as follows. In Section II the basic assumptions and definitions are discussed. This is followed by the derivation of the equations relating the current and voltage harmonics in Section III. The solution to the derived equations in a three-phase system is discussed in Section IV. Finally, the analytical results are compared with experimental results on a 10 kVA prototype in Section V.

II. Foundations for the Analysis

A. Modeling Approach and Assumptions

The estimation of the arm currents is based on the fundamental frequency component in the ac-side current, the direct current in the dc-line and the modulation index. The chosen modeling approach is to derive equations that relate the total voltage across all submodules in one phase-leg to the circulating current. The resulting current can then be calculated by specifying circuit parameters such as number of phases and dc-link filter banks.

In order to simplify the analysis some simplifications and assumptions are made. These assumptions are as follows:

1) *Only the fundamental frequency component in the pulse pattern is considered.* This is equivalent with assuming an infinite switching frequency and considerably simplifies the analysis. Hence, the focus of the analysis is to investigate the effect of the inevitable fundamental frequency component in the pulse pattern.
2) *All submodules are identical and instantaneous voltage balancing is assumed.* It is assumed that the capacitor voltages are balanced at all times. Furthermore, it is assumed that all submodules are identical. This way the need for treating the submodules individually can be avoided.
3) *Losses are modeled with a series resistance*. For simplicity, the losses that are included in the modeling are represented by a resistance that is connected in series with each arm. Leakage currents and nonlinear voltage drops across the semiconductors are not included in the model. The total resistive voltage drop across each phase leg is modeled by an effective resistance R that is distributed evenly between the upper and lower arm.
4) *Direct modulation is used.* It is assumed that the modulation is carried out by simply varying the number of submodules that are connected in each arm in a sinusoidal manner. The capacitor voltages are balanced by actively choosing which submodule to connect or bypass in each switching instant [1]. In this paper this modulation method is referred to as direct modulation. The analysis in this paper, however, aims to describe the effect of the inevitable fundamental frequency component in the pulse pattern. This means that the results can be applied for other modulation methods as well, assuming that the pulse patterns to the submodules in each arm share the same fundamental frequency component.

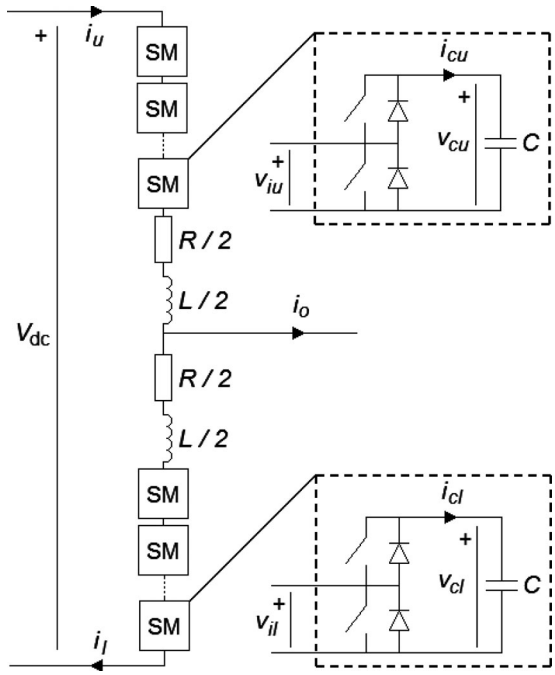

Fig. 1. One phase leg of the M2C, including the schematics of the upper and lower arm submodules.

B. Definitions

The currents, voltages, and insertion indices need to be defined in order to carry on with the calculations. One phase-leg is illustrated in Fig. 1 where the positive directions of the currents and voltages are defined.

The arm currents are defined such that a positive arm current is charging the capacitors and the alternating and direct-currents are defined as for dc/ac-inverter operation. Furthermore, the insertion indices of the upper and lower arms are denoted by

N_u and N_l, respectively. They are defined as

$$N_u = \frac{1}{2}(1 - \hat{m}\cos(\omega t)) \tag{1}$$

$$N_l = \frac{1}{2}(1 + \hat{m}\cos(\omega t)) \tag{2}$$

where $\hat{m} \in [0 \quad 1]$ is the modulation index. The insertion indices describe how many modules, on average are connected in each arm. To measure the phase angle of sinusoidal quantities a reference waveform must be chosen. The reference is chosen as

$$s_{\mathrm{ref}} = \cos(\omega t) \tag{3}$$

meaning that the time varying component in the lower arm insertion index, N_l, have zero degrees phase-shift. The choice of reference is motivated by the fact that under ideal conditions the voltage at the ac-side connection point is in phase with (3).

The arm currents can be described by the general expressions

$$i_u = \sum_{n=0}^{\infty} i_{\mathrm{un}} \tag{4}$$

$$i_l = \sum_{n=0}^{\infty} i_{\mathrm{ln}} \tag{5}$$

where

$$i_{\mathrm{un}} = \hat{i}_{\mathrm{un}}\cos(n\omega t + \phi_{\mathrm{un}}) \tag{6}$$

$$i_{\mathrm{ln}} = \hat{i}_{\mathrm{ln}}\cos(n\omega t + \phi_{\mathrm{ln}}). \tag{7}$$

The ac-side current is defined as for inverter operation, as shown in Fig. 1. Consequently, the ac-side quantities will hereafter be referred to as the output current and output voltage. As it is assumed that the output current is purely sinusoidal without any dc components, it can be defined as

$$i_o = 2\hat{i}_{\mathrm{a1}}\cos(\omega t + \phi_{\mathrm{a1}}) \tag{8}$$

where $\hat{i}_{\mathrm{a1}}$ indicates half of the peak value of the fundamental frequency component and ϕ_{a1} describes the angular displacement with respect to the reference in (3). The peak value $\hat{i}_{\mathrm{a1}}$ is defined such that if the current is split evenly between the arms, a current with the peak value $\hat{i}_{\mathrm{a1}}$ must flow in each arm toward the ac terminal.

The last quantity that has to be defined is the direct current, which is defined as the dc component of the circulating current. The circulating current can be expressed as half of the sum of the upper and lower arm currents. Thus, the dc component of the circulating current can be expressed as

$$i_{\mathrm{dc}} = \frac{1}{2}\overline{(i_u + i_l)}. \tag{9}$$

III. Deriving the Equations for Relating Current and Voltage Harmonics

A. Phase-Leg Voltage Equations

The first step to derive the expressions for the phase-leg voltage is to find the duty ratio of the submodules. As the voltage-balancing is instantaneous, all modules are identical and the switching frequency is infinite, it is easily understood that the duty ratio is proportional to the amount of connected modules in each arm. This means that the duty ratio of the submodules in one arm is equal to the insertion index for that arm. As a consequence the inserted voltage and capacitor currents are proportional to the insertion indices in each arm. Hence, the currents i_{cu} and i_{cl} in Fig. 1 can be expressed as

$$i_{\mathrm{cu}} = N_u i_u \tag{10}$$

$$i_{\mathrm{cl}} = N_l i_l. \tag{11}$$

Similarly, the voltage v_i, that is inserted by each submodule can be obtained by multiplying the insertion index with the capacitor voltage, that is

$$v_{\mathrm{iu}} = N_u v_{\mathrm{cu}} \tag{12}$$

$$v_{\mathrm{il}} = N_l v_{\mathrm{cl}}. \tag{13}$$

If the capacitance of one submodule capacitor is C, the capacitor voltages are easily found by integrating the capacitor currents i_{cu} and i_{cl}

$$v_{\mathrm{cu}} = \frac{1}{C}\int N_u i_u \, dt \tag{14}$$

$$v_{\mathrm{cl}} = \frac{1}{C}\int N_l i_l \, dt. \tag{15}$$

Inserting (1)–(2) and (4)–(5) in (14) and (15) yields

$$2Cv_{\mathrm{cu}} = \int (1 - \hat{m}\cos(\omega t))\left(\sum_{n=0}^{\infty} i_{\mathrm{un}}\right) dt \tag{16}$$

$$2Cv_{\mathrm{cl}} = \int (1 + \hat{m}\cos(\omega t))\left(\sum_{n=0}^{\infty} i_{\mathrm{ln}}\right) dt. \tag{17}$$

Any dc component in the integrands resulting from the products in the integrands would cause the capacitor voltages to grow infinitely high. Therefore, there must be no dc component in the integrand at steady-state operation. The products may, however, yield several dc components that sums to be 0.

According to (1) and (2), the average duty ratio over one fundamental period is always 0.5. Assuming that there is a dc component in the circulating current this will result in a dc component in the integrands in (16) and (17).

The output current imposes a fundamental frequency component in the arm currents. As the duty ratio is varying sinusoidally with the fundamental frequency, this will cause the capacitor current to have a dc component. This is illustrated in Fig. 2 where a 50 Hz current with the peak amplitude 1 A is switched with 1 kHz. The duty ratio is varying sinusoidally in phase with the current so that the duty ratio is higher than 0.5 during the positive half-period and less than 0.5 during the negative half period. Inevitably, this will cause the net-flow of charge to be positive, as is clearly seen in Fig. 2.

The dc components that originate from the output current and the direct current are of equal magnitude and of opposite signs. This means that for inverter operation the direct current is charging the capacitors, which are then discharged by the output current.

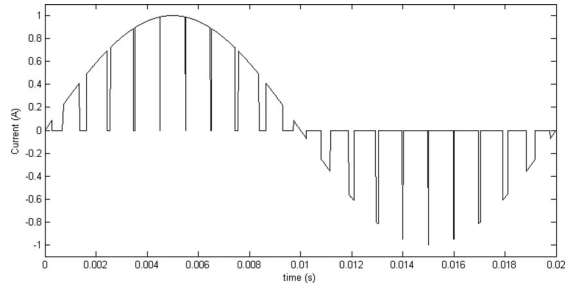

Fig. 2. Alternating current switched with a sinusoidally varying duty ratio.

The integral over one period is zero for the harmonics as well as the product of the fundamental and any given harmonic. This means that integrating the integrals in (16) and (17) over one period T simplifies the integrands substantially

$$\int_0^T (1-\hat{m}\cos(\omega t))\left(\sum_{n=0}^{\infty} i_{\mathrm{un}}\right) dt = \int_0^T \left[i_{\mathrm{u0}} - \hat{i}_{\mathrm{u1}}\hat{m}\cos(\omega t)\cos(\omega t+\phi_{\mathrm{u1}})\right] dt \quad (18)$$

$$\int_0^T (1+\hat{m}\cos(\omega t))\left(\sum_{n=0}^{\infty} i_{\mathrm{ln}}\right) dt = \int_0^T \left[i_{\mathrm{l0}} + \hat{i}_{\mathrm{l1}}\hat{m}\cos(\omega t)\cos(\omega t+\phi_{\mathrm{l1}})\right] dt. \quad (19)$$

As a consequence, for the system to be stable, the dc components of the cosine products in (18) and (19) must be equal to i_{u0} and i_{l0}. A stable system must therefore satisfy the following equations

$$i_{\mathrm{u0}} - \frac{\hat{m}\hat{i}_{\mathrm{u1}}}{2}\cos(\phi_{\mathrm{u1}}) = 0 \quad (20)$$

$$i_{\mathrm{l0}} + \frac{\hat{m}\hat{i}_{\mathrm{l1}}}{2}\cos(\phi_{\mathrm{l1}}) = 0. \quad (21)$$

Equations (20) and (21) form an underdetermined system of equations. This means that it is not possible to determine if the amplitudes of i_{u1} and i_{l1} are equal. The fundamental frequency component in the arm currents can, however, be separated in a circulating and noncirculating part

$$i_{\mathrm{u1}} = i_{\mathrm{a1}} + i_1 \quad (22)$$

$$i_{\mathrm{l1}} = -i_{\mathrm{a1}} + i_1 \quad (23)$$

where i_{a1} is half of the output current and i_1 is the circulating current at the fundamental frequency. This way the upper and lower arm currents can be expressed by components that are of equal magnitudes in both arms.

According to the assumptions that were made, the output current does not have a dc component or harmonics. Consequently, the dc component and all harmonic components in the arm currents are circulating, meaning that they are of equal magnitude and phase in both arms. The arm currents can then be redefined as

$$i_u = i_{\mathrm{dc}} + i_{\mathrm{a1}} + \sum_{n=1}^{\infty} i_n \quad (24)$$

$$i_l = i_{\mathrm{dc}} - i_{\mathrm{a1}} + \sum_{n=1}^{\infty} i_n \quad (25)$$

where

$$i_n = \hat{i}_n \cos(n\omega t + \phi_n). \quad (26)$$

The total arm voltages are found by multiplying the capacitor voltages in (14) and (15) with the number of inserted submodules. If there are N submodules in each arm the total arm voltages are given by

$$v_u = N\left(\frac{1-\hat{m}\cos(\omega t)}{2}\right)\frac{1}{C}\int N_u i_u\, dt \quad (27)$$

$$v_l = N\left(\frac{1+\hat{m}\cos(\omega t)}{2}\right)\frac{1}{C}\int N_l i_l\, dt \quad (28)$$

which can be written as

$$\frac{2Cv_u}{N} = (1-\hat{m}\cos(\omega t))\int N_u i_u\, dt \quad (29)$$

$$\frac{2Cv_l}{N} = (1+\hat{m}\cos(\omega t))\int N_l i_l\, dt. \quad (30)$$

The sum of (29) and (30) gives the total inserted voltage across the whole phase-leg, scaled by $2C$ over N, that is

$$\frac{2Cv_u}{N} + \frac{2Cv_l}{N} = (1-\hat{m}\cos(\omega t))\int N_u i_u\, dt + (1+\hat{m}\cos(\omega t))\int N_l i_l\, dt \quad (31)$$

which also can be written as

$$\frac{2C(v_u+v_l)}{N} = \int (N_u i_u + N_l i_l)\, dt - \hat{m}\cos(\omega t)\int (N_u i_u - N_l i_l)\, dt. \quad (32)$$

The products $N_u i_u$ and $N_l i_l$ are given by

$$N_u i_u = \frac{1}{2}\Big(i_{\mathrm{dc}} + i_{\mathrm{a1}} + \sum_{n=1}^{\infty} i_n - \hat{m}\cos(\omega t) i_{\mathrm{dc}} - \hat{m}\cos(\omega t) i_{\mathrm{a1}} - \hat{m}\cos(\omega t)\sum_{n=1}^{\infty} i_n\Big) \quad (33)$$

$$N_l i_l = \frac{1}{2}\Big(i_{\mathrm{dc}} - i_{\mathrm{a1}} + \sum_{n=1}^{\infty} i_n + \hat{m}\cos(\omega t) i_{\mathrm{dc}} - \hat{m}\cos(\omega t) i_{\mathrm{a1}} + \hat{m}\cos(\omega t)\sum_{n=1}^{\infty} i_n\Big). \quad (34)$$

According to (29) and (30), the dc components of the products in (33) and (34) must be 0. If they were not to be zero, the system would become unstable. As a consequence, the integral over one

period must be zero, that is

$$\frac{1}{T}\int_0^T N_u i_u\,dt = \frac{1}{2}\frac{1}{T}\int_0^T \left[i_{\rm dc} - i_{\rm a1}\hat{m}\cos(\omega t) - i_1\hat{m}\cos(\omega t)\right]dt = 0 \tag{35}$$

$$\frac{1}{T}\int_0^T N_l i_l\,dt = \frac{1}{2}\frac{1}{T}\int_0^T \left[i_{\rm dc} - i_{\rm a1}\hat{m}\cos(\omega t) + i_1\hat{m}\cos(\omega t)\right]dt = 0. \tag{36}$$

Performing the integrations yields

$$\frac{1}{T}\int_0^T N_u i_u\,dt = \frac{i_{\rm dc}}{2} - \frac{\hat{m}}{4}\hat{i}_{\rm a1}\cos(\alpha) - \frac{\hat{m}}{4}\hat{i}_1\cos(\phi_1) \tag{37}$$

$$\frac{1}{T}\int_0^T N_l i_l\,dt = \frac{i_{\rm dc}}{2} - \frac{\hat{m}}{4}\hat{i}_{\rm a1}\cos(\alpha) + \frac{\hat{m}}{4}\hat{i}_1\cos(\phi_1). \tag{38}$$

As (37) and (38) are 0, the same holds true for their difference. Subtracting (37) from (38) yields

$$\frac{1}{T}\int_0^T N_l i_l\,dt - \frac{1}{T}\int_0^T N_u i_u\,dt = \frac{1}{2}\hat{m}\hat{i}_1\cos(\phi_1) = 0 \tag{39}$$

which means that any circulating component at the fundamental frequency must be phase-shifted $\pm$ 90 degrees relative to the reference in (3). Equations (37) and (38) suggest that a circulating current that does not fulfil this criterion would cause a positive net-flow of energy to one arm and a negative net-flow of energy to the other.

The integrands in (32) are described by the sum and difference of (33) and (34), that is

$$N_u i_u + N_l i_l = i_{\rm dc} + \sum_{n=1}^{\infty} i_n - \hat{m}\cos(\omega t) i_{\rm a1} \tag{40}$$

$$N_u i_u - N_l i_l = i_{\rm a1} - \hat{m}\cos(\omega t) i_{\rm dc} - \hat{m}\cos(\omega t)\sum_{n=1}^{\infty} i_n. \tag{41}$$

Inserting (40) and (41) in (32) gives

$$\frac{2C}{N}(v_u + v_l) = Q_1 + Q_2 + Q_3 + Q_4 + Q_5 + Q_6 \tag{42}$$

where

$$Q_1 = \int i_{\rm dc}\,dt \tag{43}$$

$$Q_2 = \int \sum_{n=1}^{\infty} \hat{i}_n \cos(n\omega t + \phi_n)\,dt \tag{44}$$

$$Q_3 = -\int \hat{m}\,\hat{i}_{\rm a1}\cos(\omega t)\cos(\omega t + \phi_{\rm a1})\,dt \tag{45}$$

$$Q_4 = -\hat{m}\cos(\omega t)\int \hat{i}_{\rm a1}\cos(\omega t + \phi_{\rm a1})\,dt \tag{46}$$

$$Q_5 = \hat{m}\cos(\omega t)\int \hat{m} i_{\rm dc}\cos(\omega t)\,dt \tag{47}$$

$$Q_6 = \hat{m}\cos(\omega t)\int \hat{m}\cos(\omega t)\sum_{n=1}^{\infty}\hat{i}_n\cos(n\omega t + \phi_n)\,dt. \tag{48}$$

The next step is to perform the integrations in order to identify the frequency content. To do this, the third and sixth integrals, Q_3 and Q_6, have to be expanded as they have products of trigonometric functions in their integrands. Since the sixth integral does not fit on a single line it is split in two parts, $Q_{6\rm a}$ and $Q_{6\rm b}$

$$Q_3 = -\frac{\hat{m}\hat{i}_{\rm a1}}{2}\int \cos(\phi_{\rm a1}) + \cos(2\omega t + \phi_{\rm a1})\,dt \tag{49}$$

$$Q_{6\rm a} = \hat{m}\cos(\omega t)\sum_{n=2}^{\infty}\int \frac{\hat{m}}{2}\hat{i}_n\cos((n-1)\omega t + \phi_n)\,dt \tag{50}$$

$$Q_{6\rm b} = \hat{m}\cos(\omega t)\sum_{n=1}^{\infty}\int \frac{\hat{m}}{2}\hat{i}_n\cos((n+1)\omega t + \phi_n)\,dt \tag{51}$$

where the sum in (50) starts from $n = 2$, as it is equal to zero for $n = 1$, according to (39).

The integrations can then be performed

$$Q_1 = i_{\rm dc}t + K_1 \tag{52}$$

$$Q_2 = \sum_{n=1}^{\infty}\frac{\hat{i}_n}{n\omega}\sin(n\omega t + \phi_n) + K_2 \tag{53}$$

$$Q_3 = -\frac{\hat{m}\hat{i}_{\rm a1}}{2}\cos(\phi_{\rm a1})t - \frac{\hat{m}\hat{i}_{\rm a1}}{4\omega}\sin(2\omega + \phi_{\rm a1}) + K_3 \tag{54}$$

$$Q_4 = -\frac{\hat{m}}{\omega}\cos(\omega t)\left(\hat{i}_{\rm a1}\sin(\omega t + \phi_{\rm a1}) + K_4\right) \tag{55}$$

$$Q_5 = \frac{\hat{m}^2}{\omega}\cos(\omega t)\left(i_{\rm dc}\sin(\omega t) + K_5\right) \tag{56}$$

$$Q_{6\rm a} = \frac{\hat{m}^2}{2}\cos(\omega t)\left(\sum_{n=2}^{\infty}\left(\frac{\hat{i}_n}{(n-1)\omega} \times \sin((n-1)\omega t + \phi_n)\right) + K_{6\rm a}\right) \tag{57}$$

$$Q_{6\rm b} = \frac{\hat{m}^2}{2}\cos(\omega t)\left(\sum_{n=1}^{\infty}\left(\frac{\hat{i}_n}{(n+1)\omega} \times \sin((n+1)\omega t + \phi_n)\right) + K_{6\rm b}\right). \tag{58}$$

The constants K_n indicate the initial charge that is stored in the upper- and lower-arm capacitors. Their contribution to (42) is one dc component and one component at the fundamental frequency. The harmonics in the circulating current originates from the variations in (42), meaning that the dc component is of no interest for this analysis. For this reason the constants K_1, K_2, and K_3 can be omitted as they do not affect the frequency

content of (42), but merely add a constant that corresponds to the time average of the capacitor voltages.

The constants K_4, K_5, $K_{6\mathrm{a}}$, and $K_{6\mathrm{b}}$ originates from the integral

$$Q_4 + Q_5 + Q_6 = -\hat{m}\cos(\omega t)\int (N_u i_u - N_l i_l)\,dt. \quad (59)$$

To simplify the calculations, define

$$\int N_u i_u\,dt = F_u(t) + K_u \quad (60)$$

$$\int N_l i_l\,dt = F_l(t) + K_l \quad (61)$$

where $F(t)$ is the primitive function to the integrand and K the integration constant. Equations (60) and (61) describe the charge that is stored in one capacitor in each arm. The charge is oscillating around K_u and K_l according to the functions $F_u(t)$ and $F_l(t)$. This means that if the stored energy is equal in the upper and lower arm, K_u is equal to K_l. Assuming that the stored energy is equal in the upper and lower arm, (59) becomes

$$Q_4 + Q_5 + Q_6 = -\hat{m}\cos(\omega t)(F_u(t) - F_l(t)) \quad (62)$$

given that $K_u = K_l$, and the constants K_4, K_5, $K_{6\mathrm{a}}$, and $K_{6\mathrm{b}}$ cancel out. It can therefore be concluded that when steady-state operation is considered, all constants K_n can be omitted in the analysis.

The different frequency components can be found by first expanding the sine-products. The right-hand side of (32) can then be described by the sum of the following expressions

$$Q_1 = i_{\mathrm{dc}}t \quad (63)$$

$$Q_2 = \sum_{n=1}^{\infty}\frac{\hat{i}_n}{n\omega}\sin(n\omega t + \phi_n) \quad (64)$$

$$Q_3 = -\frac{\hat{m}\hat{i}_{\mathrm{a1}}}{2}\cos(\phi_{\mathrm{a1}})t - \frac{\hat{m}\hat{i}_{\mathrm{a1}}}{4\omega}\sin(2\omega t + \phi_{\mathrm{a1}}) \quad (65)$$

$$Q_4 = -\frac{\hat{m}\hat{i}_{\mathrm{a1}}}{2\omega}(\sin(2\omega t + \phi_{\mathrm{a1}}) + \sin(\phi_{\mathrm{a1}})) \quad (66)$$

$$Q_5 = \frac{\hat{m}^2 i_{\mathrm{dc}}}{2\omega}\sin(2\omega t) \quad (67)$$

$$Q_{6\mathrm{a}} = \frac{\hat{m}^2}{4}\sum_{n=2}^{\infty}\left(\frac{\hat{i}_n}{(n-1)\omega} \times (\sin((n-2)\omega t + \phi_n) + \sin(n\omega t + \phi_n))\right) \quad (68)$$

$$Q_{6\mathrm{b}} = \frac{\hat{m}^2}{4}\sum_{n=1}^{\infty}\left(\frac{\hat{i}_n}{(n+1)\omega} \times (\sin(n\omega t + \phi_n) + \sin((n+2)\omega t + \phi_n)\right). \quad (69)$$

Finally, the frequency content can be extracted from the derived equations. They are labeled f_n where n corresponds to the harmonic order. There are, however, two terms that are growing linearly with time. These can be found in Q_1 and Q_3 and their sum is

$$f_\infty = \left(i_{\mathrm{dc}} - \frac{\hat{m}\hat{i}_{\mathrm{a1}}}{2}\cos(\phi_{\mathrm{a1}})\right)t. \quad (70)$$

This gives a relation between the fundamental frequency component and the direct current since f_∞ must be zero for the system to be stable, that is

$$i_{\mathrm{dc}} = \frac{\hat{m}\hat{i}_{\mathrm{a1}}}{2}\cos(\phi_{\mathrm{a1}}). \quad (71)$$

Combining (20)–(23) and (71), shows that for the system to be stable, i_{a1} must fully counteract the charging or discharging process that originates from i_{dc}. This also implies that any circulating current at the fundamental frequency in steady state must be phase-shifted 90° relative to the reference in (3). If either one of the two constraints is not satisfied the system will become unstable. In one case the unbalance between the arm-voltages is growing with time, in the other case the total phase-leg voltage becomes unstable.

It is concluded that a fundamental frequency component in the circulating current can transport energy between the upper and lower arm. The circulating current changes the magnitude of the ac components in the upper and lower arms whereas the direct current remains unaffected. This means that the total energy transfer rate to the converter will remain constant, but the net-flow of energy in one arm will be positive whereas it will be negative in the other. Whether the net-flow of energy is positive or negative depends on the phase of the circulating component, as described by (37) and (38).

The component at the fundamental frequency is found in Q_2 for $n = 1$, $Q_{6\mathrm{a}}$ for $n = 3$ and $Q_{6\mathrm{b}}$ for $n = 1$. The sum of the contributions is given by

$$f_1 = \frac{\hat{m}^2}{8\omega}\hat{i}_3\sin(\omega t + \phi_3) + \frac{8 + \hat{m}^2}{8\omega}\hat{i}_1\sin(\omega t + \phi_1). \quad (72)$$

The second-order harmonic has contributions from all integrals except Q_1. Since this results in a large expression it is split up in the contributions from each different integral. Accordingly

$$f_{2\mathrm{a}} = \frac{\hat{i}_2}{2\omega}\sin(2\omega t + \phi_2) \quad (73)$$

$$f_{2\mathrm{b}} = -\frac{\hat{m}\hat{i}_{\mathrm{a1}}}{4\omega}\sin(2\omega t + \phi_{\mathrm{a1}}) \quad (74)$$

$$f_{2\mathrm{c}} = -\frac{\hat{m}\hat{i}_{\mathrm{a1}}}{2\omega}\sin(2\omega t + \phi_{\mathrm{a1}}) \quad (75)$$

$$f_{2\mathrm{d}} = \frac{\hat{m}^2\hat{i}_{\mathrm{dc}}}{2\omega}\sin(2\omega t) \quad (76)$$

$$f_{2e1} = \frac{\hat{m}^2\hat{i}_2}{4\omega}\sin(2\omega t + \phi_2) \quad (77)$$

$$f_{2e2} = \frac{\hat{m}^2\hat{i}_4}{12\omega}\sin(2\omega t + \phi_4) \quad (78)$$

$$f_{2\mathrm{f}} = \frac{\hat{m}^2\hat{i}_2}{12\omega}\sin(2\omega t + \phi_2) \quad (79)$$

where f_{2a} is the contribution from Q_2, f_{2b} is the contribution from Q_3 and so on. To give a better overview of the equations they can be sorted and gathered in three different parts

$$f_{2A} = \frac{3+2\hat{m}^2}{6\omega}\hat{i}_2 \sin(2\omega t + \phi_2) \tag{80}$$

$$f_{2B} = -\frac{3\hat{m}}{4\omega}\hat{i}_{a1} \sin(2\omega t + \phi_{a1}) + \frac{\hat{m}^2}{2\omega} i_{dc} \sin(2\omega t) \tag{81}$$

$$f_{2C} = \frac{\hat{m}^2}{12\omega}\hat{i}_4 \sin(2\omega t + \phi_4). \tag{82}$$

Finally, higher order harmonics ($n > 2$) are given by

$$f_{na} = \frac{2(n^2-1)+n^2\hat{m}^2}{2n\omega(n^2-1)}\hat{i}_n \sin(n\omega t + \phi_n) \tag{83}$$

$$f_{nb} = \frac{\hat{m}^2}{4}\left(\frac{\hat{i}_{n+2}}{(n+1)\omega}\sin(n\omega t + \phi_{n+2}) + \frac{\hat{i}_{n-2}}{(n-1)\omega}\sin(n\omega t + \phi_{n-2})\right). \tag{84}$$

Equations (72) and (80)–(84) now fully describe the harmonic content of the phase-leg voltages as functions of the arm currents.

B. Matrix Representation of the Harmonic Components

The infinite number of equations defined by (83)–(84) can be sorted by their harmonic order. By doing this it is seen that the odd and even harmonics are decoupled. According to (42) the sum of (83) and (84) is equal to the voltage variation in the phase-leg, scaled by $2C$ over N, that is

$$f_{na} + f_{nb} = \frac{2C}{N}u_n \tag{85}$$

where u_n is the nth harmonic of the phase-leg voltage. The system of equations can then be described by two matrix equations

$$\begin{bmatrix} b_2 & c_2 & & & & \\ a_4 & b_4 & c_4 & & & \\ & a_6 & b_6 & c_6 & & \\ & & a_8 & b_8 & c_8 & \\ & & & \ddots & \ddots & \ddots \end{bmatrix} \begin{bmatrix} \hat{i}_2 \\ \hat{i}_4 \\ \hat{i}_6 \\ \hat{i}_8 \\ \vdots \end{bmatrix} = \begin{bmatrix} k + \frac{2C}{N}u_2 \\ \frac{2C}{N}u_4 \\ \frac{2C}{N}u_6 \\ \frac{2C}{N}u_8 \\ \vdots \end{bmatrix} \tag{86}$$

$$\begin{bmatrix} b_1 & c_1 & & & & \\ a_3 & b_3 & c_3 & & & \\ & a_5 & b_5 & c_5 & & \\ & & a_7 & b_7 & c_7 & \\ & & & \ddots & \ddots & \ddots \end{bmatrix} \begin{bmatrix} \hat{i}_1 \\ \hat{i}_3 \\ \hat{i}_5 \\ \hat{i}_7 \\ \vdots \end{bmatrix} = \begin{bmatrix} \frac{2C}{N}u_1 \\ \frac{2C}{N}u_3 \\ \frac{2C}{N}u_5 \\ \frac{2C}{N}u_7 \\ \vdots \end{bmatrix} \tag{87}$$

where

$$a_n = \frac{\hat{m}^2}{4(n-1)\omega}\sin(n\omega t + \phi_{n-2}) \tag{88}$$

$$b_n = \frac{2(n^2-1)+n^2\hat{m}^2}{2n\omega(n^2-1)}\sin(n\omega t + \phi_n) \tag{89}$$

$$c_n = \frac{\hat{m}^2}{4(n+1)\omega}\sin(n\omega t + \phi_{n+2}) \tag{90}$$

except for b_1 which is given by

$$b_1 = \left(\frac{8+\hat{m}^2}{8\omega}\right)\hat{i}_1 \cos(\omega t + \phi_1) \tag{91}$$

and

$$k = \frac{3\hat{m}\hat{i}_{a1}}{4\omega}\sin(2\omega t + \phi_{a1}) - \frac{\hat{m}^2 i_{dc}}{2\omega}\sin(2\omega t). \tag{92}$$

To simplify the calculations, complex representation of the currents can be used. All currents and voltages are then defined by

$$i_n = Re\{\hat{i}_n e^{j\phi_n} e^{jn\omega t}\} \tag{93}$$

$$u_n = Re\{\hat{u}_n e^{j\phi_{vn}} e^{jn\omega t}\}. \tag{94}$$

Matrices E_e, E_o, X_e, and X_o are defined as

$$E_e = \begin{bmatrix} e^{j2\omega t} & & & \\ & e^{j4\omega t} & & \\ & & e^{j6\omega t} & \\ & & & \ddots \end{bmatrix} \tag{95}$$

$$E_o = \begin{bmatrix} e^{j1\omega t} & & & \\ & e^{j3\omega t} & & \\ & & e^{j5\omega t} & \\ & & & \ddots \end{bmatrix} \tag{96}$$

$$X_e = \begin{bmatrix} y_2 & z_2 & & & \\ x_4 & y_4 & z_4 & & \\ & x_6 & y_6 & z_6 & \\ & & \ddots & \ddots & \ddots \end{bmatrix} \tag{97}$$

$$X_o = \begin{bmatrix} y_1 & z_1 & & & \\ x_3 & y_3 & z_3 & & \\ & x_5 & y_5 & z_5 & \\ & & \ddots & \ddots & \ddots \end{bmatrix} \tag{98}$$

where

$$x_n = -j\frac{\hat{m}^2}{\omega 4(n-1)} \tag{99}$$

$$y_n = -j\frac{2(n^2-1)+n^2\hat{m}^2}{2n\omega(n^2-1)} \tag{100}$$

$$z_n = -j\frac{\hat{m}^2}{\omega 4(n+1)} \tag{101}$$

except for y_1 which is given by

$$y_1 = -j\frac{8+\hat{m}^2}{8\omega}. \tag{102}$$

Equations (86) and (87) can then be expressed as

$$E_e X_e \begin{bmatrix} \hat{i}_2 e^{j\phi_2} \\ \hat{i}_4 e^{j\phi_4} \\ \hat{i}_6 e^{j\phi_6} \\ \vdots \end{bmatrix} = \begin{bmatrix} (r+q_2)e^{j2\omega t} \\ q_4 e^{j4\omega t} \\ q_6 e^{j6\omega t} \\ \vdots \end{bmatrix} \tag{103}$$

$$E_o X_o \begin{bmatrix} \hat{i}_1 e^{j\phi_1} \\ \hat{i}_3 e^{j\phi_3} \\ \hat{i}_5 e^{j\phi_5} \\ \vdots \end{bmatrix} = \begin{bmatrix} q_1 e^{j1\omega t} \\ q_3 e^{j3\omega t} \\ q_5 e^{j5\omega t} \\ \vdots \end{bmatrix} \tag{104}$$

where

$$q_n = \frac{2C}{N}\hat{u}_n e^{j\phi_{vn}} \tag{105}$$

$$r = -j\left(\hat{i}_{\mathrm{a1}}\frac{3\hat{m}}{4\omega}e^{j\phi_{\mathrm{a1}}} - \frac{\hat{m}^2 i_{\mathrm{dc}}}{2\omega}\right). \tag{106}$$

Equations in (103) and (104) are time-variant. This can be solved by multiplying both sides of the equations with the inverse of E_e and E_o. The equations relating the currents i_n to the voltages u_n can then be expressed as

$$\begin{bmatrix} y_2 & z_2 & & & \\ x_4 & y_4 & z_4 & & \\ & x_6 & y_6 & z_6 & \\ & & \ddots & \ddots & \ddots \end{bmatrix} \begin{bmatrix} \hat{i}_2 e^{j\phi_2} \\ \hat{i}_4 e^{j\phi_4} \\ \hat{i}_6 e^{j\phi_6} \\ \vdots \end{bmatrix} = \begin{bmatrix} r+q_2 \\ q_4 \\ q_6 \\ \vdots \end{bmatrix} \tag{107}$$

$$\begin{bmatrix} y_1 & z_1 & & & \\ x_3 & y_3 & z_3 & & \\ & x_5 & y_5 & z_5 & \\ & & \ddots & \ddots & \ddots \end{bmatrix} \cdot \begin{bmatrix} \hat{i}_1 e^{j\phi_1} \\ \hat{i}_3 e^{j\phi_3} \\ \hat{i}_5 e^{j\phi_5} \\ \vdots \end{bmatrix} = \begin{bmatrix} q_1 \\ q_3 \\ q_5 \\ \vdots \end{bmatrix}. \tag{108}$$

IV. Solving the Equations

The solution to (107) and (108) depends on circuit specific quantities such as dc-link filter parameters, harmonics in the dc-line current, and number of phases. For simplicity it is assumed that the dc-line current is a pure direct current, implying that all current harmonics are absorbed by the dc-link filter. The filter is modeled as an impedance Z_f connected in parallel with the phase-legs (including the arm impedances).

A. Three-Phase System

The arm impedances in the three-phase converter can be regarded as a Y-connected load with a neutral connection through the impedance Z_f. This is illustrated in Fig. 3 where the cascaded submodules are put in boxes labeled "phase-leg." These

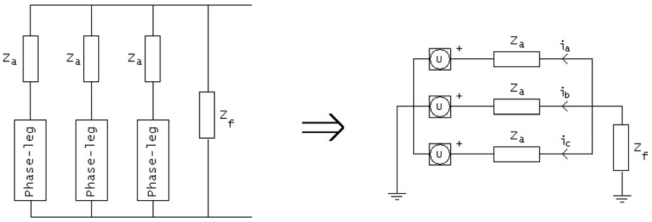

Fig. 3. For the ac components in the dc-link current, the dc-link is modeled as an open circuit with a filter impedance.

phase-legs are regarded as ideal, that is, there are no resistive or inductive elements inside the phase-leg boxes. The arm resistances and inductances are connected in series with the phase-legs. The sum of the upper and lower arm impedance is given by

$$Z_a = R + jn\omega L \tag{109}$$

where R is the effective resistance in the whole phase leg and L is the sum of the upper and lower arm inductances. The resistance R and inductance L are evenly distributed between the upper and lower arms as shown in Fig. 1.

Positive and negative sequence voltages do not result in any currents through the filter impedance Z_f. The zero sequence components, however, do. Both Z_f and Z_a can be described as arbitrary impedances. For simplicity, Z_f is considered to be purely capacitive and Z_a is assumed to be resistive– inductive. The positive and negative sequence components are then given by

$$u_n = -(jn\omega L + R)\left(\hat{i}_n e^{j(n\omega t+\phi_n)}\right) \tag{110}$$

whereas negative sequence components are given by

$$u_{n(z)} = -\left(jn\omega L + R + \frac{3}{jn\omega C_f}\right)\left(\hat{i}_n e^{j(n\omega t+\phi_n)}\right). \tag{111}$$

The elements q_n in (105) can then be expressed as

$$q_n = -\frac{2C}{N}(jn\omega L + R)\hat{i}_n e^{j\phi_n} \tag{112}$$

when n is not a multiple of three, in which case the equation for the zero sequence components must be used

$$q_{n(z)} = -\frac{2C}{N}\left(jn\omega L - j\frac{3}{n\omega C_f} + R\right)\hat{i}_n e^{j\phi_n}. \tag{113}$$

Equations (107) and (108) can then be written as

$$\begin{bmatrix} v_2 & z_2 & & & \\ x_4 & v_4 & z_4 & & \\ & x_6 & v_6 & z_6 & \\ & & \ddots & \ddots & \ddots \end{bmatrix} \cdot \begin{bmatrix} \hat{i}_2 e^{j\phi_2} \\ \hat{i}_4 e^{j\phi_4} \\ \hat{i}_6 e^{j\phi_6} \\ \vdots \end{bmatrix} = \begin{bmatrix} r \\ 0 \\ 0 \\ \vdots \end{bmatrix} \tag{114}$$

$$\begin{bmatrix} v_1 & z_1 & & & \\ x_3 & v_3 & z_3 & & \\ & x_5 & v_5 & z_5 & \\ & & \ddots & \ddots & \ddots \end{bmatrix} \cdot \begin{bmatrix} \hat{i}_1 e^{j\phi_1} \\ \hat{i}_3 e^{j\phi_3} \\ \hat{i}_5 e^{j\phi_5} \\ \vdots \end{bmatrix} = \begin{bmatrix} 0 \\ 0 \\ 0 \\ \vdots \end{bmatrix} \tag{115}$$

where

$$v_n = y_n + \frac{2C}{N}(jn\omega L + R) \tag{116}$$

for nontripplen values of n and

$$v_{n(z)} = y_n + \frac{2C}{N}\left(jn\omega L - j\frac{3}{n\omega C_f} + R\right) \tag{117}$$

when n is a multiple of 3. As y_n is purely imaginary for all n, the real part of v_n is always $2RC$ over N. It can therefore be concluded that none of the diagonal elements in (115) is 0. As a consequence it is concluded that there are no odd harmonics in the arm currents as the solution to (115) is the zero-vector.

B. General Solution

1) Resonant Frequencies: The imaginary part of v_n may become zero for certain values of ω, indicating resonant behaviour of the converter. The resonance affects the circulating current as i_n is determined by the weighted sum of i_{n-2} and i_{n+2} divided by v_n, that is

$$i_n = -\frac{x_n i_{n-2} + z_n i_{n+2}}{v_n}. \tag{118}$$

The real part of v_n consists of only the resistance R. Ideally, the resistance is very small in order to achieve a high efficiency of the converter. The amplitude of the circulating current i_n in (118) may therefore become very high for the angular frequency $\omega = \omega_{rn}$

$$w_{rn} = \sqrt{\frac{N}{LC}}\sqrt{\frac{2(n^2-1)+\hat{m}^2n^2}{4n^2(n^2-1)}} \quad n = 3k \pm 1. \tag{119}$$

The resonant frequencies that are associated with the zero sequence components in (117) are not considered as they are in the kilohertz range for reasonable values of L, C, and C_f.

The resonant frequency ω_{rn} is the fundamental frequency for which the amplitude of the nth harmonic is only limited by the resistance R. This means that every harmonic is associated with its own resonant frequency. Equation (119) also indicates that this frequency is decreasing, approximately as 1 over n, for higher order harmonics. The damping effect of R is, however, increasing with higher order harmonics as x_n and z_n are decreasing in magnitude while R remains constant.

In order not to rely on the resistance R, which should be kept as low as possible from an efficiency point of view, it is therefore favourable to operate the converter above the highest resonant frequency given by (119). The highest resonant frequency in (119) is obtained with $n = 2$ and $m = 1$. This gives the following constraints on the capacitors and arm inductors

$$LC > \frac{5N}{24\omega^2} \tag{120}$$

where ω is the fundamental frequency in radians per second.

2) Circulating Current: The second-order harmonic can be solved from (114) as

$$\hat{i}_2 e^{j\phi_2} = \frac{r}{g_2} \tag{121}$$

where g_2 is given by the recursive expression

$$g_{n-2} = v_{n-2} - z_{n-2}\frac{x_n}{g_n} \tag{122}$$

where $g_n \to v_n$ as $n \to \infty$. Inserting (106) in (121) gives

$$\hat{i}_2 e^{j\phi_2} = -\frac{j}{g_2}\left(\hat{i}_{\mathrm{a}1}\frac{3\hat{m}}{4\omega}e^{j\phi_{\mathrm{a}1}} - \frac{\hat{m}^2 i_{\mathrm{dc}}}{2\omega}\right). \tag{123}$$

By substituting i_{dc} into (71), (123) can be expressed as

$$\hat{i}_2 e^{j\phi_2} = -\frac{j}{g_2}\left(\frac{3e^{j\phi_{\mathrm{a}1}} - \hat{m}^2\cos(\phi_{\mathrm{a}1})}{4\omega}\right)\hat{i}_{\mathrm{a}1}. \tag{124}$$

The value of g_2 is a function of the circuit parameters, modulation index, and fundamental frequency, but does not depend on the current $i_{\mathrm{a}1}$. This means that the relation between the ac-side current and the second-order harmonic in the circulating current, given by (124), is valid for all systems. It is concluded that the second-order harmonic is directly proportional to the amplitude of the ac-side current. The proportionality constant depends on the load angle $\phi_{\mathrm{a}1}$ and reaches its minimum value at purely active power transfer. Similarly, higher order harmonics can be calculated as

$$\hat{i}_n e^{j\phi_n} = \frac{-x_n \hat{i}_{\mathrm{n}-2} e^{j\phi_{\mathrm{n}-2}}}{g_n}. \tag{125}$$

C. Approximative Solutions when $C_f \to \infty$

When the dc-link is modeled as a constant voltage source, an approximate solution can be found by using $g_n \approx v_n$ for any $n \geq 2$ in (122). Equation (118) gives

$$\hat{i}_n \leq \left|\frac{x_n}{v_n}\right|\hat{i}_{n-2} + \left|\frac{z_n}{v_n}\right|\hat{i}_{n+2} \tag{126}$$

which can be expressed as

$$\hat{i}_n \leq \left(\left|\frac{x_n}{v_n}\right| + \left|\frac{z_n}{v_n}\right|\right)\hat{i}_{n-2} + \left|\frac{z_n}{v_n}\right|\left(\hat{i}_{n+2} - \hat{i}_{n-2}\right). \tag{127}$$

From (99) and (101) it is obvious that x_n and z_n are decreasing with higher values of n. Conversely, the magnitude of v_n is increasing, assuming that (120) is satisfied. As a consequence, if (120) is satisfied, and the constraint

$$\left|\frac{x_n}{v_n}\right| + \left|\frac{z_n}{v_n}\right| < 1 \tag{128}$$

is satisfied for $n = 4$, it is also satisfied for all even values of $n \geq 4$. Assuming that the constraint in (128) is satisfied, (127) indicates that the magnitude of the harmonics are either strictly increasing or strictly decreasing. This can be shown by first expressing (127) as

$$\hat{i}_n - \left(\left|\frac{x_n}{v_n}\right| + \left|\frac{z_n}{v_n}\right|\right)\hat{i}_{n-2} \leq \left|\frac{z_n}{v_n}\right|\left(\hat{i}_{n+2} - \hat{i}_{n-2}\right). \tag{129}$$

Applying (128) on (129) gives

$$\hat{i}_n - \hat{i}_{n-2} < \left|\frac{z_n}{v_n}\right|\left(\hat{i}_{n+2} - \hat{i}_{n-2}\right). \tag{130}$$

This means that if $\hat{i}_n > \hat{i}_{n-2}$, then $\hat{i}_{n+2} > \hat{i}_n$ since

$$\left|\frac{z_n}{v_n}\right| < 1 \tag{131}$$

according to (128). It can be concluded that the amplitude of the harmonics are strictly decreasing, as the opposite would cause the harmonics to approach infinity with higher values of n. As a consequence, the maximum possible amplitude of the harmonics can be expressed as

$$\hat{i}_n < \left(\left|\frac{x_n}{v_n}\right| + \left|\frac{z_n}{v_n}\right|\right)\hat{i}_{n-2} \tag{132}$$

assuming that (120) and (128) are satisfied.

1) Including Only the Second-Order Harmonic: According to (114), the second-order harmonic can be expressed as

$$v_2\hat{i}_2 e^{j\phi_2} + z_2\hat{i}_4 e^{j\phi_4} = r. \tag{133}$$

In some cases an approximative solution can be obtained directly from (133). That is, if

$$\frac{\left|v_2\hat{i}_2 e^{j\phi_2}\right|}{\left|z_2\hat{i}_4 e^{j\phi_4}\right|} \gg 1 \tag{134}$$

the second-order harmonic can be approximated as

$$\hat{i}_2 e^{j\phi_2} \approx \frac{r}{v_2}. \tag{135}$$

If (120) and (128) are satisfied, (132) can be applied on (134). The constraint in (134) can then be expressed as

$$\frac{|v_2|}{|z_2|\left(\left|\frac{x_4}{v_4}\right| + \left|\frac{z_4}{v_4}\right|\right)} \gg 1. \tag{136}$$

This is used in the experimental results in order to determine if (135) can be used to describe the second-order harmonic in the circulating current.

2) Including an Arbitrary Number of Harmonics: By combining (118) and (125) it is found that

$$g_n = \frac{x_n v_n i_{n-2}}{x_n i_{n-2} + z_n i_{n+2}}. \tag{137}$$

It is concluded that the approximation $g_n \approx v_n$ can be used for any n that satisfies

$$\frac{|x_n i_{n-2}|}{|z_n i_{n+2}|} \gg 1. \tag{138}$$

Assuming that (120) and (128) are satisfied, it is possible to apply (132) on (138) and the constraint can then be expressed as

$$\frac{|x_n|}{|z_n|\left(\frac{|x_{n+2}|}{|v_{n+2}|} + \frac{|z_{n+2}|}{|v_{n+2}|}\right)\left(\frac{|x_n|}{|v_n|} + \frac{|z_n|}{|v_n|}\right)} \gg 1. \tag{139}$$

The harmonics in the circulating current can then be obtained from (122) and (125) by using $g_n \approx v_n$ for the first n that satisfies (139).

D. Boundary Value as $C_f \to 0$

If the capacitance C_f approaches zero, the zero sequence harmonics i_{zs} approaches zero, assuming that the system remains stable as C_f approaches 0. The second and fourth harmonics can then be solved from (114) since $\hat{i}_6 = 0$

$$\begin{bmatrix} v_2 & z_2 \\ x_4 & v_4 \end{bmatrix}\begin{bmatrix} \hat{i}_2 e^{j\phi_2} \\ \hat{i}_4 e^{j\phi_4} \end{bmatrix} = \begin{bmatrix} r \\ 0 \end{bmatrix} \tag{140}$$

that is

$$\hat{i}_2 e^{j\phi_2} = \frac{v_4 r}{v_2 v_4 - z_2 x_4} \tag{141}$$

$$\hat{i}_4 e^{j\phi_4} = -\frac{x_4 r}{v_2 v_4 - z_2 x_4}. \tag{142}$$

Higher order harmonics can be calculated directly from (114) as every tripplen harmonic is 0. Consequently, i_8 can be calculated from i_6, i_{10} can be calculated from i_8 and so on.

V. Experimental Results

The experiments are carried out on a 10 kVA three-phase prototype with five submodules per arm. The converter is operated in inverter mode with a passive load, and is connected to a 500 V dc supply. The optimal choice of arm inductors and submodule capacitors depends on the intended application and current ratings. The prototype was designed with 3.3 mF submodule capacitors and 4.7 mH arm inductors. These values are not optimized for this specific experiment, but the validity of the theoretical findings does not depend on optimized circuit parameters. The effective arm resistance is unknown and the given capacitance is not very accurate. These two parameters can, however, be measured by applying the analytical results on the measured data. This is done in the first experiment in order to obtain more accurate values of R and C.

Direct modulation is used to control the converter. That is, reference values are generated for the number of inserted modules in the upper and lower arms. The fractional parts of the reference values are compared with a 5 kHz triangular carrier. This way the actual number of submodules that are connected can be varied between the two nearest integer values in a pulse width modulation like manner. To balance the capacitor voltages, the insertion and bypassing of submodules is done according to the sorting algorithm that was presented in [1].

A. Resonant Frequency and Parameter Measurements

The analytical results suggest that there is a resonant frequency, for which the second order harmonic in the circulating current peaks. The fundamental frequency at which resonance occurs for the second order harmonic can be estimated by inserting the approximate values of L and C in (119). With the modulation index $\hat{m} = 0.9$, the fundamental frequency where this occurs is expected to be approximately 28 Hz. This was investigated by varying the fundamental frequency from 15 to 50 Hz in steps of 1 Hz while keeping the modulation index constant at 0.9. A purely resistive load was used in order to maintain a constant load during the experiment.

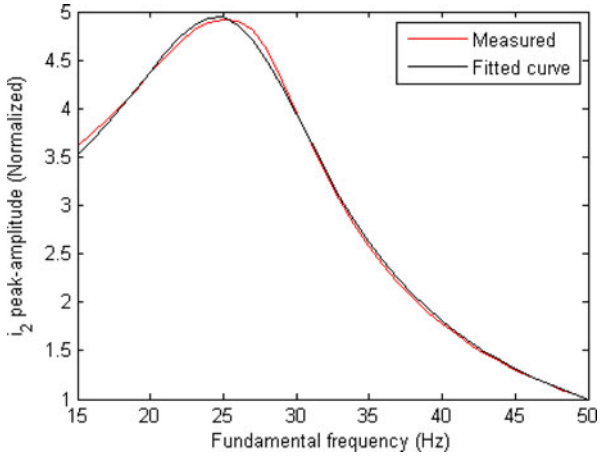

Fig. 4. Parameter values were extracted by least square fitting to the measured curve.

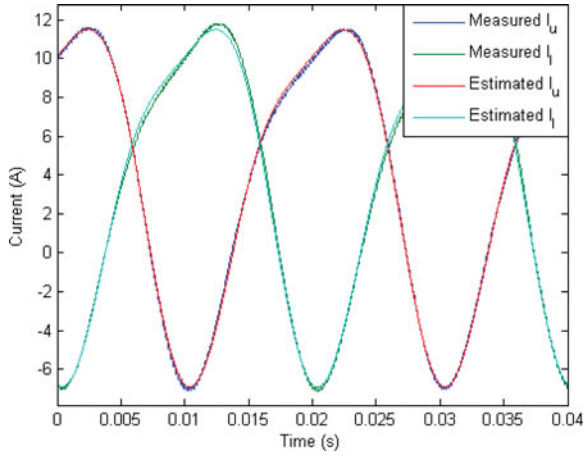

Fig. 5. Measured and calculated upper and lower arm currents.

The measured amplitudes of the second-order harmonic in the circulating current are shown in Fig. 4. The amplitudes have been normalized such that the value is 1 at 50 Hz. The expected peak is easily identified at 25 Hz, this is lower than the expected value which indicates that the actual capacitance of the capacitors is slightly higher than the given approximate value.

The values of the resistance R and capacitance C can be extracted from the measured data by least square fitting of the analytical expression to the measured curve. It is then found that the effective resistance R in the phase leg is 1.8 Ω, and the capacitance of the capacitors is 3.64 mF. The fitted curve is shown in Fig. 4 together with the measured values.

B. Estimating the Arm Currents

By using the extracted values of R and C, x, z, and v in (132) can be calculated. It is then found that the harmonic content in the circulating current is dominated by the second-order harmonic as the amplitude of i_4 is at least 47 times smaller than the amplitude of i_2. Furthermore, it can be concluded that the second-order harmonic can be calculated with (135) as the left-hand side of (136) is in the order of 10^3.

Inserting (106) and (100) in (135) gives

$$i_2 = Re\left\{\frac{-j\left(\hat{i}_{\mathrm{a1}}\frac{3\hat{m}}{4\omega}e^{j\phi_{\mathrm{a1}}} - \frac{\hat{m}^2 i_{\mathrm{dc}}}{2\omega}\right)}{\frac{2C}{N}(j2\omega L + R) - j\frac{6+4\hat{m}^2}{12\omega}}e^{j2\omega t}\right\}. \tag{143}$$

The upper and lower arm currents can then be calculated as

$$i_u = i_{\mathrm{dc}} + \frac{1}{2}i_o + i_2 \tag{144}$$

$$i_l = i_{\mathrm{dc}} - \frac{1}{2}i_o + i_2 \tag{145}$$

where the direct current i_{dc} and output current i_o are obtained from the measurements.

The converter was set to supply a passive resistive–inductive load. With the modulation index 0.9 the measured ac-side current was 12.4 A rms, 13° inductive. The analytical waveforms are compared with the actual currents in Fig. 5. The analytical and experimental results agree well and the estimated currents are almost identical to the measured arm currents. It is concluded that (143) predicts the correct phase and amplitude of the second-order harmonic in the circulating current. The prediction that the harmonic contents are dominated by the second-order harmonic is also in good agreement with the experimental results.

VI. Conclusion

The analytical results describe the harmonic contents in the arm currents resulting from the fundamental frequency component in the pulse patterns to the submodules. The validity of the analytical equations was confirmed by experiments on a 10 kVA prototype with 30 submodules. An interesting outcome of the analysis was that there are resonant frequencies for which a given harmonic is only limited by the losses in the system, which was also verified experimentally. If this is not taken in to consideration it could cause problems in systems with high efficiencies. The derived equations for the harmonic components can be very useful in the design of a modular multilevel converter. The results not only point out which values of the arm inductances and submodule capacitances must be avoided, but also the benefit to increasing either the inductance or capacitance in terms of harmonics in the arm currents.

The arm inductances and submodule capacitances can be chosen such that the nominal frequency is above the relevant resonant frequencies. This way operating the converter close to any resonant frequency at nominal operation can be avoided. In some applications such as motor drives it may, however, be desirable to operate the converter at very low frequencies. As a consequence, operating the converter at any of the resonant frequencies cannot be fully avoided. This must be considered in the system design and development of a suitable controller for high-performance motor drives.

REFERENCES

[1] A. Lesnicar and R. Marquardt, "An innovative modular multilevel converter topology suitable for a wide power range," in *Proc. IEEE Bologna Power Tech*, 2012, vol. 3, 2003, p. 6.

[2] A. Lesnicar and R. Marquardt, "A new modular voltage source inverter topology," in *Proc. Eur. Conf. Power Electron. Appl*., 2003, pp. 1–10.

[3] R. Marquardt and A. Lesnicar, "New concept for high voltage-modular multilevel converter," in *Proc. Power Electron. Spec. Conf.*, 2004, pp. 174–179.

[4] M. Glinka and R. Marquardt, "A new ac/ac multilevel converter family," *IEEE Trans. Ind. Electron*., vol. 52, no. 3, pp. 662–669, Jun. 2005.

[5] S. Allebrod, R. Hamerski, and R. Marquardt, "New transformerless, scalable modular multilevel converters for HVDC-transmission," in *Proc. IEEE Power Electron. Spec. Conf*., 2008, pp. 174–179.

[6] D. Peftitsis, G. Tolstoy, A. Antonopoulos, J. Rabkowski, J.-K. Lim, M. Bakowski, L. Angquist, and H.-P. Nee, "High-power modular multilevel converters with SiC JFETs," in *Proc. IEEE Energy Convers. Congr. Expo*., 2010, pp. 2148–2155.

[7] M. Hiller, D. Krug, R. Sommer, and S. Rohner, "A new highly modular medium voltage converter topology for industrial drive applications," in *Proc. Eur. Conf. Power Electron. Appl*., 2009, pp. 1–10.

[8] A. Antonopoulos, K. Ilves, L. Angquist, and H.-P. Nee, "On interaction between internal converter dynamics and current control of high-performance high-power ac motor drives with modular multilevel converters," in *Proc. IEEE Energy Convers. Congr. Expo*., 2010, pp. 4293–4298.

[9] M. Hagiwara, K. Nishimura, and H. Akagi, "A medium-voltage motor drive with a modular multilevel PWM inverter," *IEEE Trans. Power Electron*., vol. 25, no. 7, pp. 1786–1799, July 2010.

[10] A. J. Korn, M. Winkelnkemper, and P. Steimer, "Low output frequency operation of the modular multi-level converter," in *Proc. IEEE Energy Convers. Congr. Expo*., 2010, pp. 3993–3997.

[11] M. Winkelnkemper, A. Korn, and P. Steimer, "A modular direct converter for transformerless rail interties," in *Proc. IEEE Int. Ind. Electron. Symp*., 2010, pp. 562–567.

[12] S. Rohner, S. Bernet, M. Hiller, and R. Sommer, "Modulation, losses, and semiconductor requirements of modular multilevel converters," *IEEE Trans. Ind. Electron*., vol. 57, no. 8, pp. 2633–2642, Aug. 2010.

[13] A. Antonopoulos, L. Angquist, and H.-P. Nee, "On dynamics and voltage control of the modular multilevel converter," in *Proc. Eur. Conf. Power Electron. Appl*., 2009, pp. 1–10.

[14] A. Rasic, U. Krebs, H. Leu, and G. Herold, "Optimization of the modular multilevel converters performance using the second harmonic of the module current," in *Proc. Eur. Conf. Power Electron. Appl*., 2009, pp. 1–10.

[15] L. Angquist, A. Antonopoulos, D. Siemaszko, K. Ilves, M. Vasiladiotis, and H.-P. Nee, "Inner control of modular multilevel converters - An approach using open-loop estimation of stored energy," in *Proc. Int. Power Electron. Conf*., 2010, pp. 1579–1585.

[16] M. Hagiwara and H. Akagi, "Control and experiment of pulsewidth-modulated modular multilevel converters," *IEEE Trans. Power Electron*., vol. 24, no. 7, pp. 1737–1746, Jul. 2009.

[17] S. Rohner, S. Bernet, M. Hiller, and R. Sommer, "Pulse width modulation scheme for the modular multilevel converter," in *Proc. Eur. Conf. Power Electron. Appl*., Jul. 2009, pp. 1–10.

[18] D. Siemaszko, A. Antonopoulos, K. Ilves, M. Vasiladiotis, L. Angquist, and H.-P. Nee, "Evaluation of control and modulation methods for modular multilevel converters," in *Proc. Int. Power Electron. Conf.*, 2010, pp. 746–753.

Kalle Ilves (S'10) received the M.Sc. degree in electrical engineering from the Royal Institute of Technology, Stockholm, Sweden, in 2009. Since 2010 he is working toward the Ph.D. degree at the department of Electrical Machines and Power Electronics, Royal Institute of Technology.

His main research interests includes high power converters for grid applications.

Antonios Antonopoulos (S'06) was born in Athens, Greece, in 1984. He received the M.Sc. degree in electrical and computer engineering from the National Technical University of Athens, Greece, in 2007. Since 2008 he is working toward the Ph.D. degree at Electrical Machines and Power Electronics Laboratory, Royal Institute of Technology, Stockholm, Sweden.

His main scientific interests include high-power electronic converters for large and medium scale motor drives and grid applications.

Staffan Norrga (M'00) was born in Lidingö, Sweden, in 1968. He received the M.Sc. degree in applied physics from Linköping Institute of Technology, Linköping, Sweden, in 1993 and the Ph.D. degree in electrical engineering from the Royal Institute of Technology, Stockholm, Sweden, in 2005.

From 1994 and 2000, he worked as a Development Engineer at ABB in Västers, Sweden, in various powerelectronics-related areas such as railway traction systems and converters for HV DC power transmission systems. Between 2000 and 2005, he returned to academia to engage in research on new power electronic converters employing soft switching and medium frequency transformers, at the Department of Electric Machines and Power Electronics of the Royal Institute of Technology. He is currently with ABB Corporate Research, Stockholm, and also with the Royal Institute of Technology. He is the inventor or co-inventor of 14 patent filings and has authored or co-authored more than 15 scientific papers published at international conferences or in journals. His research interests include new converter topologies for power transmission applications and grid integration of renewable energy sources.

Hans-Peter Nee (S'91–M'96–SM'04) was born in Västers, Sweden, in 1963. He received the M.Sc., Licentiate, and Ph.D. degrees in electrical engineering from the Royal Institute of Technology, Stockholm, Sweden, in 1987, 1992, and 1996, respectively.

In 1999, he was appointed a Professor of Power Electronics in the Department of Electrical Machines and Power Electronics, Royal Institute of Technology. His research interests include power electronic converters, semiconductor components, and control aspects of utility applications, such as FACTS and HVDC, and variable-speed drives.